

Accepted Manuscript

CRISPR-Cas9-mediated disruption of the HMG-CoA reductase genes of *Mucor circinelloides* and subcellular localization of the encoded enzymes

Gábor Nagy, Amanda Grace Vaz, Csilla Szebenyi, Miklós Takó, Eszter J. Tóth, Árpád Csernetics, Ottó Bencsik, András Szekeres, Mónika Homa, Ferhan Ayaydin, László Galgóczy, Csaba Vágvölgyi, Tamás Papp

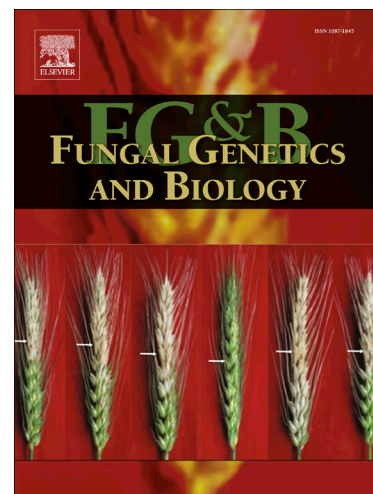
PII: S1087-1845(19)30011-8
DOI: <https://doi.org/10.1016/j.fgb.2019.04.008>
Reference: YFGBI 3221

To appear in: *Fungal Genetics and Biology*

Received Date: 8 January 2019
Revised Date: 11 April 2019
Accepted Date: 12 April 2019

Please cite this article as: Nagy, G., Grace Vaz, A., Szebenyi, C., Takó, M., Tóth, E.J., Csernetics, A., Bencsik, O., Szekeres, A., Homa, M., Ayaydin, F., Galgóczy, L., Vágvölgyi, C., Papp, T., CRISPR-Cas9-mediated disruption of the HMG-CoA reductase genes of *Mucor circinelloides* and subcellular localization of the encoded enzymes, *Fungal Genetics and Biology* (2019), doi: <https://doi.org/10.1016/j.fgb.2019.04.008>

This is a PDF file of an unedited manuscript that has been accepted for publication. As a service to our customers we are providing this early version of the manuscript. The manuscript will undergo copyediting, typesetting, and review of the resulting proof before it is published in its final form. Please note that during the production process errors may be discovered which could affect the content, and all legal disclaimers that apply to the journal pertain.



CRISPR-Cas9-mediated disruption of the HMG-CoA reductase genes of *Mucor circinelloides* and subcellular localization of the encoded enzymes

Gábor Nagy^{a,b§}, Amanda Grace Vaz^{a,b§}, Csilla Szebenyi^{a,b,c}, Miklós Takó^c, Eszter J. Tóth^{a,b},
Árpád Csernetics^{a,c}, Ottó Bencsik^c, András Szekeres^c, Mónika Homa^{a,c}, Ferhan Ayaydin^d,
László Galgóczy^e, Csaba Vágvolgyi^{b,c}, Tamás Papp^{a,b,c*}

^aMTA-SZTE “Lendület” Fungal Pathogenicity Mechanisms Research Group, Közép fasor 52., 6726 Szeged, Hungary

^bInterdisciplinary Excellence Centre, Department of Microbiology, University of Szeged, Közép fasor 52., 6726 Szeged, Hungary

^cDepartment of Microbiology, Faculty of Science and Informatics, University of Szeged, Közép fasor 52., 6726 Szeged, Hungary

^dLaboratory of Cellular Imaging, Biological Research Centre, Hungarian Academy of Sciences, Temesvári krt. 62., 6726 Szeged, Hungary

^eInstitute of Plant Biology, Biological Research Centre, Hungarian Academy of Sciences, Temesvári krt. 62., 6726 Szeged, Hungary

[§]Authors Gábor Nagy and Amanda Grace Vaz contributed equally to this work.

*Correspondence:

Dr. Tamás Papp

pappt@bio.u-szeged.hu

ABSTRACT

Terpenoid compounds, such as sterols, carotenoids or the prenyl groups of various proteins are synthesized via the mevalonate pathway. A rate-limiting step of this pathway is the conversion of 3-methylglutaryl-CoA (HMG-CoA) to mevalonic acid catalyzed by the HMG-CoA reductase. Activity of this enzyme may affect several biological processes, from the synthesis of terpenoid metabolites to the adaptation to various environmental conditions. In this study, the three HMG-CoA reductase genes (i.e. *hmgR1*, *hmgR2* and *hmgR3*) of the β -carotene producing filamentous fungus, *Mucor circinelloides* were disrupted individually and simultaneously by a recently developed *in vitro* plasmid-free CRISPR-Cas9 method. Examination of the mutants revealed that the function of *hmgR2* and *hmgR3* are partially overlapping and involved in the general terpenoid biosynthesis. Moreover, *hmgR2* seemed to have a special role in the ergosterol biosynthesis. Disruption of all three genes affected the germination ability of the spores and the sensitivity to hydrogen peroxide. Disruption of the *hmgR1* gene had no effect on the ergosterol production and the sensitivity to statins but caused a reduced growth at lower temperatures. By confocal fluorescence microscopy using strains expressing GFP-tagged HmgR proteins, all three HMG-CoA reductases were localized in the endoplasmic reticulum.

Keywords: CRISPR-Cas9, mevalonate pathway, ergosterol, carotenoids, statins, endoplasmic reticulum

1. Introduction

Fungal sterols and other terpenoids are synthesized via the mevalonate pathway. This biosynthetic route leads to the formation of dimethylallyl pyrophosphate and isopentenyl pyrophosphate, which are the common precursors of the various terpenoid compounds. A crucial step of this pathway is the conversion of 3-hydroxy-3-methylglutaryl coenzyme A (HMG-CoA) to mevalonic acid catalyzed by the HMG-CoA reductase (Fig.1). This is a membrane anchored enzyme, which is generally located in the endoplasmic reticulum (ER) but other subcellular localizations, such as in the mitochondria or peroxisomes, may also occur (Koning et al., 1996; Breitling and Krisans, 2002; Vaupotič and Plemenitas, 2007).

Playing a central role in the formation of the different terpenoid compounds (i.e. ergosterol, dolichol, carotenoids or the prenyl components of ubiquinone and several proteins), activity of the HMG-CoA reductase may affect various biological processes, such as the pigment production, morphogenesis, maintenance of the cell integrity and adaptation to environmental changes, especially to fluctuating oxygen tension and osmotic conditions (Wang and Keasling, 2002; Seong et al., 2006; Verwaal et al., 2007; Bidle et al., 2007; Vaupotič et al., 2008; Yan et al., 2012; Nagy et al., 2014). Inhibition of the enzyme or disruption of the encoding gene decreased the virulence of various plant and human pathogenic fungi, such as *Aspergillus fumigatus*, *Candida albicans* or *Fusarium graminearum* (Seong et al., 2006; Tashiro et al., 2012; Leal et al., 2013), indicating that HMG-CoA reductase may also affect the pathogenicity. Moreover, ergosterol and its biosynthesis are currently among the most important targets of antifungal therapy, therefore, ergosterol biosynthesis and its regulation are intensively studied areas (Macreadie et al., 2006; Burg and Espenshade, 2011; Andrade-Pavón et al., 2013).

The β -carotene producing *Mucor circinelloides* f. *lusitanicus* is a frequently used model organism to study, among others, morphogenesis and morphological dimorphism (Lee

et al., 2015; Valle-Maldonado et al., 2015), RNA interference in the fungal cell (Nicolás et al., 2015), production of enzymes, carotenoids and other metabolites (Papp et al., 2016), as well as the genetic background of pathogenicity of Mucoralean fungi (Li et al., 2011; Lee et al., 2013). The genome of this fungus contains three different HMG-CoA reductase genes, namely, *hmgR1*, *hmgR2* and *hmgR3*. Previously, transcription of all three genes was proven by real-time quantitative reverse transcription PCR (qRT-PCR) and the overexpression of *hmgR2* and *hmgR3* was found to affect the carotenoid production of the fungus (Nagy et al., 2014). In the present study, the *hmgR* genes of *M. circinelloides* were disrupted separately and simultaneously applying a recently described plasmid-free CRISPR-Cas9 method developed for Mucoromycota fungi (Nagy et al., 2017). The resulting transformants were used to characterize the function of the different HmgRs. In parallel, subcellular localization of green fluorescent protein (GFP)-fused enzymes was studied by confocal fluorescence microscopy.

2. Materials and methods

2.1 Strains, media and growth conditions

M. circinelloides f. *lusitanicus* MS12 strain derived from *M. circinelloides* f. *lusitanicus* CBS 277.49 by chemical mutagenesis (Benito et al., 1992) was used in the transformation experiments. This strain is auxotrophic to leucine and uracil (*leuA*⁻ and *pyrG*⁻) but wild-type for carotene and ergosterol biosynthesis. For nucleic acid, carotenoid and ergosterol extraction, 10⁶ sporangiospores were plated onto solid minimal medium (YNB; 10 g/L glucose, 0.5 g/L yeast nitrogen base without amino acids (Difco), 1.5 g/L (NH₄)₂SO₄, 1.5 g/L sodium glutamate and 20 g/L agar) supplemented with leucine and/or uracil (0.5 g/L) if required and incubated at 25 °C for 4 days. To measure the colony diameters and analyze the macro- and micromorphology, 10⁵ sporangiospores were inoculated onto the center of solid

YNB plates. The diameter of the colonies was measured daily after incubating the plates at 15, 20, 25, 30 and 35 °C using the MS12 strain as the growth control. To analyze their viability and germinating ability, sporangiospores were inoculated into 30 ml liquid YNB to reach the final density of 10^5 spores/mL and were incubated for 6 h at 25 °C under continuous shaking at 200 rpm. To examine the stability of the mutants under non-selective conditions, malt extract agar medium (MEA; 10 g/L glucose, 5 g/L yeast extract, 25 ml/L 20% malt extract and 20 g/L agar) was used.

2.2 General molecular techniques

Genomic DNA was purified by using the ZR Fungal/Bacterial DNA MiniPrep kit (Zymo Research). PCR products were isolated and concentrated using the Zymoclean Large Fragment DNA Recovery Kit (Zymo Research) and the DNA Clean & Concentrator-5 (Zymo Research). Oligonucleotide sequences were designed based on the sequence data available in the *M. circinelloides* CBS277.49v2.0 genome database (DoE Joint Genome Institute; <http://genome.jgi-psf.org/Mucci2/Mucci2.home.html>) (Corrochano et al., 2016). Primers used in the PCR and the qRT-PCR experiments are listed in Supplementary Table S1.

2.3 Design of the gRNAs and construction of the disruption cassettes to disrupt the *hmgR* genes by the CRISPR-Cas9 method

The protospacer sequences designed to target the DNA cleavage in the *hmgR1*, *hmgR2* and *hmgR3* genes were the followings, 5'-cacatagcgtgtttacgcac-3'; 5'-ctctgatatcgtacgccct-3' and 5'-accacgatcattactgctga-3', respectively, which correspond to the fragments of the nucleotide positions between 1994 and 2013 downstream from the start codon of the *hmgR1* gene, between the positions 2117 and 2137 downstream from the start codon of *hmgR2* and between the positions 2571 and 2590 downstream from the start codon of *hmgR3*, respectively. Using

these sequences, the Alt-R CRISPR crRNA and Alt-R CRISPR-Cas9 tracrRNA molecules were designed and purchased from Integrated DNA Technologies (IDT). To form the crRNA:tracrRNA duplexes (i.e. the gRNAs), the Nuclease-Free Duplex Buffer (IDT) was used according to the instructions of the manufacturer.

Genome editing strategies (Fig. 2) followed the set-up described recently (Nagy et al., 2017). HDR was applied for all gene disruptions following the strategy described previously (Nagy et al., 2017). Disruption cassettes functioning also as the template DNA for the HDR were constructed by PCR using the Phusion Flash High-Fidelity PCR Master Mix (Thermo Scientific). In case of the *hmgR1* gene, at first, two fragments being 1712 and 1958 nucleotides upstream and downstream from the protospacer sequence and the *M. circinelloides pyrG* gene (CBS277.49v2.0 genome database ID: Mucci1.e_gw1.3.865.1) along with its promoter and terminator sequences were amplified using the primer pairs h1p1-h1p2 and h1p3-h1p4, respectively (see Supplementary Table S1). The amplified fragments were fused in a subsequent PCR using the nested primers h1p7 and h1p8 (see Supplementary Table S1); the ratio of the fragments in the reaction was 1:1:1. Disruption of *hmgR2* using the *pyrG* gene was carried out previously (Nagy et al., 2017). This gene was also disrupted using the *leuA* gene (CBS277.49v2.0 genome database ID: Mucci1.e_gw1.2.132.1) as follows: two fragments, which were 1817 and 1698 nucleotides upstream and downstream from the protospacer sequence, respectively, were fused with the *leuA* gene by PCR using the nested primers h2p7 and h2p8 (see Supplementary Table S1). In case of *hmgR3*, two fragments, 1800 and 2012 nucleotides upstream and downstream from the protospacer sequence, respectively, were fused with *pyrG* or *leuA* by PCR using nested primers h3p7 and h3p8 (see Supplementary Table S1).

2.4 Construction of plasmids for the expression of the GFP-tagged proteins

To construct the vectors for the expression of the GFP-fused HmgR proteins, the plasmids pNG1, pNG2 and pNG3 were used, which harbor the *hmgR1*, *hmgR2* and *hmgR3* genes, respectively, under the control of the glucose-inducible *M. circinelloides gpd1* (glyceraldehyde-3-phosphate dehydrogenase 1) promoter (Nagy et al., 2014). The *gfp* gene was ligated in frame with *hmgR1* at the restriction sites *NheI-NotI* of pNG1, which contained the coding region of the 1-553 amino acids of HmgR1, arising pH1cGFP. To construct pH2cGFP and pH3cGFP, *gfp* was ligated in frame at the restriction sites *EcoRI-NotI* of pNG2 containing the coding region of the 1-756 amino acids of HmgR2 and pNG3 containing the coding region of the 1-825 amino acids of HmgR3, respectively. By this way, the *hmgR* genes were truncated and the catalytic domains of the enzymes were replaced to *gfp*. In the final constructs, expression of each GFP-fused gene was driven by the *Mucor gpd1* promoter.

2.5 Transformation experiments

For both the CRISPR-Cas9-mediated gene disruption and the introduction of the plasmids expressing the GFP-fused proteins, the PEG-mediated protoplast transformation method was used according to van Heeswijk and Roncero (1984). Protoplasts were prepared as described earlier (Nagy et al., 1994).

For a single gene disruption by the CRISPR-Cas9 method, 5 μ g template DNA (disruption cassette), 10 μ M gRNA and 10 μ M Cas9 nuclease were added to the protoplasts in one transformation reaction as described by Nagy et al. (2017). To perform double gene disruptions, 20 μ M gRNA and 20 μ M Cas9 enzyme were applied and 5 μ g of each template DNA was added to the transformation reaction.

In case of the plasmids pH1cGFP, pH2cGFP and pH3cGFP, 3 μ g DNA was added to the protoplasts in a transformation reaction. From each transformation experiment, 10-10 transformant colonies were isolated. Fluorescent microscopy analysis demonstrated that all of

them expressed the corresponding GFP-fused proteins (i.e. HmgR1:GFP, HmgR2:GFP and HmgR3:GFP).

In each case, transformants were selected on solid YNB medium by the complementation of the uracil and/or the leucin auxotrophy of the MS12 strain. From each primary transformant, monosporangial colonies were formed under selective conditions.

2.6 qRT-PCR analysis

RNA was purified using the Direct-zol RNA miniprep kit (Zymo Research) or the TRI Reagent (Sigma-Aldrich) according to the instructions of the manufacturers. Reverse transcription was carried out with the Maxima H Minus First Strand cDNA Synthesis Kit (Thermo Scientific) using random hexamer and oligo(dT)18 primers, following the manufacturer's instructions. The qRT-PCR experiments were performed in a CFX96 real-time PCR detection system (Bio-Rad) using the Maxima SYBR Green qPCR Master Mix (Thermo Scientific) and the primers presented in Supplementary Table S1. The relative quantification of the copy number and the gene expression was carried out by the $2^{-\Delta\Delta Ct}$ method using the actin gene (scaffold_07: 2052804-2054242) of *M. circinelloides* as a reference. All experiments were performed in three biological and technical parallels.

2.7 Isolation and examination of the membrane fraction

For isolation of the membrane fraction, the mycelium was harvested from the surface of solid YNB medium and was disrupted in a mortar using liquid nitrogen. Eight ml homogenization buffer (250 mM sucrose, 1 mM EDTA, 10 mM Tris-HCl; pH 7.2) was added to each 4 g of the mycelium. Homogenized samples were incubated for 10 min at 4 °C and centrifuged for 15 min at 500×g. The supernatant was transferred to an ultracentrifuge tube and centrifuged for 1 h at 100,000×g at 4 °C. After this procedure, the supernatant containing the soluble

proteins was discarded, while the pellet containing the insoluble membrane fraction was resuspended in 1 ml homogenization buffer. The fluorescence signal was measured using a fluorimeter (FLUOstar OPTIMA, BMG Labtech) where the excitation filter was 485 BP and the emission filter was 500-10. The homogenization buffer was used as the background control.

2.8 Fluorescence microscopy

To stain the ER, the mitochondria, and the lipid droplets, Er-Tracker Red (BODIPY TR Glibenclamide; Life Technologies), MitoTracker Red FM (Life Technologies) and Nile Res (Thermo Scientific) were used according to the instructions of the manufacturer.

To examine the viability of the strains, the FUN 1 dye (Thermo Scientific) was used according to the instructions of the manufacturer. To determine the ratio of metabolically active and non-active cells, ten fields of view were counted by fluorescent microscopy. The experiment was performed in three independent replicates.

In case of light- and fluorescence microscopy analyses, an AxioLab (Carl Zeiss) fluorescence microscope equipped with an AxioCam ERc 5 (Carl Zeiss) camera was used. Filter set 15 (excitation BP 546/12, emission LP 590; Carl Zeiss) was applied to examine the propidium-iodide staining and filter set 9 (excitation BP 450-490, emission LP 515; Carl Zeiss) was used to detect the Annexin V-FITC staining and the GFP signal. A FluoView FV1000 (Olympus) confocal microscope was used to examine the localization of the GFP signal (excitation 488, emission 510) and the ER-Tracker and MitoTracker Red staining (excitation 543, emission 603).

2.9 Susceptibility tests

Susceptibility of the fungal strains to hydrogen peroxide was examined in a 96-well microtiter plate assay. Hydrogen peroxide was diluted in liquid YNB to prepare a stock solution of 100 mM. Final concentrations of the hydrogen peroxide in the wells ranged from 0 to 10 mM. Dilutions and inocula were prepared in liquid YNB. The final density of sporangiospores in the wells was set to 10^4 . Plates were incubated for 48 h at 25 °C and the optical density of the fungal cultures was measured at 620 nm using a Jupiter HD plate reader (ASY5 Hitech). The uninoculated medium was used as the background for the calibration and the fungal growth in the hydrogen peroxide-free medium was considered as 100%; all experiments were performed in triplicates.

Susceptibility of the original and the mutant strains to fluvastatin, atorvastatin and rosuvastatin was examined in a broth microdilution assay as described earlier (Nagy et al., 2014). Minimal inhibitory concentration (MIC) of the statins was determined as the lowest concentration of the tested compound that caused at least 90% growth inhibition compared to the drug-free control medium.

2.10 Analysis of the carotenoid and ergosterol content

Carotenoid and ergosterol extraction and HPLC analyses were performed as described earlier (Nagy et al., 2014).

2.11 Homology modelling

Homology models of *M. circinelloides* HmgR1, HmgR2 and HmgR3 were generated with I-TASSER using their amino acid sequences as templates (UniProt IDs: A0A168LXB4, A0A168P835, A0A168MWS8, respectively) (Yang et al., 2015). The models with highest confidence scores were refined with ModRefiner (Xu and Zhang, 2011), and visualized with UCSF Chimera software (Pettersen et al., 2001). Accuracy of the protein model prediction

was analyzed at RAMPAGE server with generation of Ramachandran plot and investigation of residues in the most favored and allowed positions (Lovell et al., 2003). Contents of the .pdb files are available in Supplementary Dataset S1-S3.

2.12 Statistical analysis

All measurements were performed in at least two technical and three biological replicates. Significance was calculated with paired t-test using Microsoft Excel of the Microsoft Office package. P values less than 0.05 were considered as statistically significant.

3. Results

3.1 Subcellular localization of HMG-CoA reductase proteins

In all GFP-fused HMG-CoA reductase expressing transformants, the green fluorescent signals co-localized with the Er-Tracker Red stain indicating the accumulation of the fusion proteins in the ER (Fig. 3). At the same time, the GFP signals were not detected in other organelles. To investigate whether the GFP-fused proteins were accumulated in the lumen or the membrane of the ER, membrane and soluble fractions were isolated from the examined strains.

Fluorescence of the membrane fraction was found to be increased with 66-80% compared to that of the untransformed MS12 strain. At the same time, we could not detect any GFP fluorescence in the soluble fractions of the transformants.

3.2 Disruption of the *hmgR* genes using the CRISPR-Cas9 method

Disruption of *hmgR2* by homology directed repair (HDR) resulting in the strain MS12- Δ *hmgR2* was reported previously (Nagy et al., 2017). For the single disruption of *hmgR1* (MS12- Δ *hmgR1*) and *hmgR3* (MS12- Δ *hmgR3*), transformation frequencies were 2 and 4 colonies per 10^5 protoplasts, respectively, while those for the simultaneous disruption of the

gene pairs *hmgR1* - *hmgR2* (MS12- Δ *hmgR1*- Δ *hmgR2*) and *hmgR1* - *hmgR3* (MS12- Δ *hmgR1*- Δ *hmgR3*) were found to be 3 and 7 colonies per 10^6 protoplasts, respectively.

Simultaneous disruption of *hmgR2* and *hmgR3* was carried out several times. In these experiments, five small and extremely slow-growing colonies were isolated but all of them died after four days. Maintenance of these colonies by transferring the mycelium or the spores onto a fresh selective medium also remained unsuccessful indicating that the simultaneous failure of these genes is a lethal condition. In case of the successful experiments, the genome editing efficiency was 100% as it was demonstrated by the PCR analysis of the mutant strains amplifying the expected fragments in each case (Fig. 4A, C, E, G, I). Mutants proved to be mitotically stable retaining the integrated fragment even after 20 cultivation cycles. qRT-PCR analysis proved the absence of the transcripts of the disrupted genes and revealed that the relative transcript level of the intact *hmgR* genes increased significantly in all mutants (Fig. 4B, D, F, H, J).

3.3 Effect of the *hmgR* gene disruptions on the carotenoid and ergosterol production

Total carotenoid content of all mutants proved to be similar to those of the original MS12 strain (476 ± 65 μ g/g [dry weight]) being in the range of 457-495 μ g/g [dry weight]. Ergosterol content also did not change significantly in the mutants MS12- Δ *hmgR1*, MS12- Δ *hmgR3* and MS12- Δ *hmgR1*- Δ *hmgR3* compared to the MS12 strain. At the same time, ergosterol content of MS12- Δ *hmgR1*- Δ *hmgR2* strains (3.18 mg/g [dry weight]) was found to be significantly decreased ($p=0.037$) but not completely ceased compared to the original strain (4.57 mg/g [dry weight]). Similarly, a decreased ergosterol content (3.27 mg/g [dry weight]) was measured previously in MS12- Δ *hmgR2* (Nagy et al., 2017).

3.4 Effect of the *hmgR* gene disruptions on the susceptibility to statins and hydrogen peroxide

Sensitivity of the *hmgR* disrupted mutants and the MS12 strain were determined to fluvastatin, atorvastatin, rosuvastatin and hydrogen peroxide by using the broth microdilution method (Table 1). Transformants, except the MS12- Δ *hmgR1* strain, showed increased susceptibility to statins. Simultaneous disruption of *hmgR1* and *hmgR2*, as well as that of the *hmgR1* and *hmgR3* resulted in similar sensitivity to statins as the single disruption of *hmgR2* and *hmgR3*, respectively. Sensitivity to hydrogen peroxide increased in all mutants and this effect was the most prominent in the MS12- Δ *hmgR1*- Δ *hmgR3* strain (Table 1).

3.5 Effect of the *hmgR* gene disruptions on the viability and the germination of the sporangiospores

FUN 1 viability assay indicated that the percentage of the metabolically active spores decreased in case of the mutants, in which either the *hmgR2* or the *hmgR3* gene was disrupted alone or together with the *hmgR1* (Fig. 5A).

At 5 h postinoculation, the spores of all types of mutants displayed moderate but statistically significantly reduced germination compared to those of MS12. This was the most explicit in case of the MS12- Δ *hmgR1*- Δ *hmgR3* mutant (Fig. 5B).

3.6 Effect of the *hmgR* gene disruptions on the colony growth

At the optimum growth temperature of *M. circinelloides* (i.e. 28 °C), colony growth of the mutants did not differ significantly from that of the MS12 strain, except in the case of the MS12- Δ *hmgR1*- Δ *hmgR3* mutant, which displayed significantly decreased colony diameter than the MS12 strain (Fig. 6). At the same time, all mutants, in which *hmgR1* had been disrupted alone or together with another gene (i.e. Δ *hmgR1*, Δ *hmgR1*- Δ *hmgR2*, and Δ *hmgR1*- Δ *hmgR3*), had significantly reduced colony diameters at 15 and 20 °C compared to the original MS12 (Fig. 6).

3.7 *In silico* homology modelling of HmgR proteins

In silico homology modelling experiments revealed that the active site containing the HMG-CoA and NADPH binding sites forms a compact, closed structure in HmgR1, while this site is open and accessible for ligands in HmgR2 and HmgR3 (Fig. 7). These predicted putative structures are highly reliable: Ramachandran plot analysis indicated that 81.2% and 12.5% of the residues are located in the favored and allowed regions for HmgR1, respectively. These values were found to be 82.4% and 12.78% at HmgR2 and 85.7% and 10.5% at HmgR3.

4. Discussion

Function of HMG-CoA reductase and its role in the various biological processes have been poorly characterized in Mucorales fungi. Previously, the presence and expression of three *hmgR* genes were demonstrated in *M. circinelloides* (Lukács et al. 2009, Nagy et al., 2014) and the comparison of their sequences showed the genes *hmgR2* and *hmgR3* closer to each other than to *hmgR1* (Lukács et al. 2009). Other members of the genus may have one, two or more *hmgR* genes (Ruiz-Albert et al., 2002; Lukács et al. 2009; Nagy et al. 2014). Based on molecular phylogenetic studies, it can be suggested that a gene duplication occurred in an ancestor of the Mucorales, which was followed by subsequent duplication and gene loss events (Ruiz-Albert et al., 2002; Lukács et al. 2009; Nagy et al. 2014). Whole genome sequencing of *M. circinelloides* and *Phycomyces blakesleeanus* revealed that an extensive genome duplication occurred before the divergence of these fungi, which contributed to the expansion of several gene families (Corrochano et al., 2016).

All three HMG-CoA reductases of *M. circinelloides* were found to be anchored to the ER membrane. In most organisms, HMG-CoA reductase is also associated to the ER but there are several exceptions (Learned and Fink, 1989; Stermer et al., 1994; Breitling and Krisans,

2002; Leivar et al., 2005; Vaupotič and Plemenitas, 2007). For instance, in human, two isoforms of the HMG-CoA reductase are expressed, one is localized in the ER and the other is in the matrix of the peroxisome (Liscum et al., 1985; Breitling and Krisans, 2002). Similarly, only one of the two HmgR enzymes of the halotolerant black yeast, *Hortaea werneckii* is localized in the ER, while the other can be found in the mitochondria (Vaupotič and Plemenitas, 2007). The genome of *Arabidopsis thaliana* encodes two HMG-CoA reductase genes and from them three isoforms are expressed and localized in the ER, the mitochondria and the chloroplasts (Learned and Fink, 1989; Stermer et al., 1994; Leivar et al., 2005).

Subcellular localization of this protein is well studied in *Saccharomyces cerevisiae*, which has two HMG-CoA reductases, both associated to the ER playing a significant role in the ER proliferation and the adaptation to anaerobiosis (Koning et al., 1996).

Based on feeding experiments with C¹⁴-labeled precursors in the *M. circinelloides*-related species *P. blakesleanus* and *Blakeslea trispora*, it was previously concluded that β -carotene and ergosterol are synthesized in different subcellular compartments using separate precursor pools from the earliest biosynthetic steps (Kuzina et al., 2006). This would suggest different localizations for the HMG-CoA reductases participating in the carotenoid and the ergosterol biosynthesis. However, our results indicate that, at least in *M. circinelloides*, all the three enzymes have the same localization in the ER raising the possibility that the different terpenoid compounds are not synthesized in independent specific compartments.

Disruption of the *hmgR2* gene of *M. circinelloides* was previously carried out by a plasmid-free CRISPR-Cas9 approach (Nagy et al., 2017). The same technique has now been used to disrupt the other two genes, *hmgR1* and *hmgR3* and to create double disruption mutants. This is the first time when multiple mutations have been induced by the CRISPR-Cas9 method in a Mucoromycota fungus. To disrupt the genes, extensive parts of them were replaced by the *pyrG* or the *leuA* genes, which complement uracil or leucine auxotrophy of the applied strain,

respectively, using the HDR method (i.e. by using a template DNA for the gene replacement). As previously observed (Nagy et al., 2017), this method caused low mutation frequency (1-4 colonies per 10^5 protoplasts) but a 100% genome editing efficiency in each experiment.

In each disruption mutant, transcription of the intact genes increased. This phenomenon suggests that the regulation of the three genes is, at least partly, coordinated and their increased activity can compensate the missing expression of the disrupted gene. In this regard, it seems that *hmgR2* and *hmgR3* have a special role in the metabolism of *M. circinelloides* as their simultaneous disruption proved to be lethal for the fungus. Earlier, transcription analysis and overexpression of the *hmgR* genes indicated that the function of these two genes is partially overlapping and both have role in the general terpenoid biosynthesis, especially in the formation of β -carotene and ergosterol (Nagy et al., 2014). A similar situation was observed in *S. cerevisiae*. Here, the simultaneous deletion of the HMG-CoA reductase genes was also found to be lethal while the functionality of one of the two genes was enough for the survival of the cell (Basson et al., 1986; Seong et al., 2006).

In contrast to the previous finding that overexpression of *hmgR2* and *hmgR3* led to elevated carotenoid content (Nagy et al., 2014), disruption of the *hmgR* genes had no effect on the carotenoid production. This was also observed in case of *hmgR2* previously (Nagy et al., 2017). We assume that a possible explanation of this contradiction can be the compensatory effect of the non-disrupted genes.

Disruption of *hmgR2* decreased the ergosterol content in agreement with the previous analysis of the gene (Nagy et al., 2017), and its overexpression also affected the ergosterol level (Nagy et al., 2014). Although the compensatory effect of the other genes was also observed, these results indicate that *hmgR2* has a primary role in the ergosterol biosynthesis.

Statins are competitive inhibitors of HMG-CoA reductase and widely used cholesterol lowering agents (Minder et al., 2012). It is known that they may have antifungal effect

(Macreadie et al., 2006; Galgóczy et al., 2009) and it has recently been found that they can decrease the virulence of *Rhizopus oryzae*, the most frequent causative agent of mucormycoses (Bellanger et al., 2016). Partial silencing of the *hmgR* gene in *Trichoderma harzianum* resulted in increased sensitivity to lovastatin and decreased ergosterol content (Cardoza et al., 2007). Previously, overexpression of *hmgR2* and *hmgR3* decreased the sensitivity of *M. circinelloides* to statins while similar effects for *hmgR1* were not detected (Nagy et al., 2014). In agreement with this, only the disruption of *hmgR2* and *hmgR3* increased the susceptibility of *M. circinelloides* to statins in the present study. Homology modelling revealed that the HMG-CoA binding site of the HmgR1 protein differs from those of HmgR2 and HmgR3, having a compact and closed structure. This structural difference can explain that the lack of HmgR1 had no effect on the susceptibility to statins and may indicate a function rather different from that of the other two enzymes.

All mutants showed an increased sensitivity to hydrogen peroxide and this effect was the most explicit in the double disruption mutants. This indicates that the activity of all three genes may have role in the adaptation to oxidative stress and their effects seem to be additive in this respect. This effect of the HMG-CoA reductases can be indirect through their possible role in the structure of the ER or in the formation of ergosterol, the prenyl group of certain proteins (such as Ras and Rho) and other terpenoid compounds participating in the defense from and adaptation to oxidative stress. Ergosterol content affects the membrane permeability, which plays an important role in the adaptation to oxidative stress (Higgins et al., 2003; Branco et al., 2004). In fact, decreased ergosterol level in *S. cerevisiae* associated with an increased sensitivity to oxidative stress (Vincent et al., 2003; Marisco et al., 2011). In *M. circinelloides*, disruption of *hmgR2* and *hmgR3* had a more explicit effect on the hydrogen peroxide sensitivity than that of *hmgR1*. This may also suggest the significance of the ergosterol content respecting this feature.

Mutants with disrupted *hmgR2* or *hmgR3* genes had less metabolically active spores than the parental strain. This observation reinforces the suggestion that, among the three genes, *hmgR2* and *hmgR3* have the principal role in the general isoprenoid biosynthesis and the production of ergosterol. Disruption of *hmgR1* had no effect on the viability of the spores. This observation agrees with a previous finding that *hmgR1* is transcribed only in the hyphae and not in the spores (Nagy et al., 2014). At the same time, disruption of all three genes affected the germination of the spores. Simultaneous disruption of *hmgR1* and *hmgR3* affected the germination of spores and the colony growth in the highest extent compared to the other mutants. Interestingly, disruption of the *hmgR1* genes also affected the colony growth at temperatures lower than the optimum. Previously, intensity of the transcription of this gene showed a clear temperature dependence and transcript abundance showed a steady relative decrease with the increasing growth temperatures (Nagy et al., 2014).

5. Conclusion

Potential roles of the three *hmgR* genes in *M. circinelloides* are presented in Fig. 8. Based on the results presented in this study, we found some overlaps among their functions, especially in case of *hmgR2* and *hmgR3*. These two genes may have a primary role in the biosynthesis of ergosterol and other isoprenoid compounds while *hmgR1* seems to be involved in the adaptation to lower temperatures.

Acknowledgements

This study was supported by the “Lendület” Grant of the Hungarian Academy of Sciences (LP2016-8/2016) and the Hungary grant 20391-3/2018/FEKUSTRAT of the Ministry of Human Capacities. Research of LG and MT was supported by the János Bolyai Research Scholarship of the Hungarian Academy of Sciences.

Competing Interests: The authors declare that they have no competing interests.

References

- Andrade-Pavón, D., Sánchez-Sandoval, E., Rosales-Acosta, B., Ibarra, J.A., Tamariz, J., Hernández-Rodríguez, C., Villa-Tanaca, L., 2013. The 3-hydroxy-3-methylglutaryl-coenzyme-A reductases from fungi: A proposal as a therapeutic target and as a study model. *Rev. Iberoam. Micol.* 31, 81-85. <https://doi.org/10.1016/j.riam.2013.10.004>.
- Basson, M.E., Thorsness, M., Rine, J., 1986. *Saccharomyces cerevisiae* contains two functional genes encoding 3-hydroxy-3-methylglutaryl-coenzyme a reductase. *Proc. Natl. Acad. Sci. USA* 83, 5563-5567.
- Bellanger, A.P., Tataru, A.M., Shirazi, F., Gebremariam, T., Albert, N.D., Lewis, R.E., Ibrahim, A.S., Kontoyiannis, D.P., 2016. Statin concentrations below the minimum inhibitory concentration attenuate the virulence of *Rhizopus oryzae*. *J. Infect. Dis.* 214, 114-121. <https://doi.org/10.1093/infdis/jiw090>.
- Benito, E.P., Díaz-Mínguez, J.M., Iturriaga, E.A., Camouzano, E.A., Eslava, A.P., 1992. Cloning and sequence analysis of the *Mucor circinelloides pyrG* gene encoding orotidine-5'-monophosphate decarboxylase: use of *pyrG* for homologous transformation. *Gene* 116, 59-67. [https://doi.org/10.1016/0378-1119\(92\)90629-4](https://doi.org/10.1016/0378-1119(92)90629-4).

Bidle, K. A., Hanson, T. E., Howell, K., Nannen, J., 2007. HMG-CoA reductase is regulated by salinity at the level of transcription in *Haloflex volcanii*. *Extremophiles* 11, 49-55. <https://doi.org/10.1007/s00792-006-0008-3>.

Branco, M.R., Marinho, H.S., Cyrne, L., Antunes, F., 2004. Decrease of H₂O₂ plasma membrane permeability during adaptation to H₂O₂ in *Saccharomyces cerevisiae*. *J. Biol. Chem.* 279, 6501-6506. <https://doi.org/10.1074/jbc.M311818200>.

Breitling, R., Krisans, S.K., 2002. A second gene for peroxisomal HMG-CoA reductase? A genomic reassessment. *J. Lipid Res.* 43, 2031-2036. <https://doi.org/10.1194/jlr.R200010-JLR200>.

Burg, J.S., Espenshade, P.J., 2011. Regulation of HMG-CoA reductase in mammals and yeast. *Prog. Lipid Res.* 50, 403-410. <https://doi.org/10.1016/j.plipres.2011.07.002>.

Cardoza, R.E., Hermosa, M.R., Vizcaíno, J.A., González, F., Llobell, A., Monte, E., Gutiérrez, S., 2007. Partial silencing of a hydroxy-methylglutaryl-CoA reductase-encoding gene in *Trichoderma harzianum* CECT 2413 results in a lower level of resistance to lovastatin and lower antifungal activity. *Fungal Genet. Biol.* 44, 269-283. <https://doi.org/10.1016/j.fgb.2006.11.013>.

Corrochano, L.M., Kuo, A., Marcet-Houben, M., Polaino, S., Salamov, A., Villalobos-Escobedo, J.M., Grimwood, J., Álvarez, M.I., Avalos, J., Bauer, D., Benito, E.P., Benoit, I., Burger, G., Camino, L.P., Cánovas, D., Cerdá-Olmedo, E., Cheng, J.F., Domínguez, A., Eliáš, M., Eslava, A.P., Glaser, F., Gutiérrez, G., Heitman, J., Henrissat, B., Iturriaga, E.A., Lang,

B.F., Lavín, J.L., Lee, S.C., Li, W., Lindquist, E., López-García, S., Luque, E.M., Marcos, A.T., Martin, J., McCluskey, K., Medina, H.R., Miralles-Durán, A., Miyazaki, A., Muñoz-Torres, E., Oguiza, J.A., Ohm, R.A., Olmedo, M., Orejas, M., Ortiz-Castellanos, L., Pisabarro, A.G., Rodríguez-Romero, J., Ruiz-Herrera, J., Ruiz-Vázquez, R., Sanz, C., Schackwitz, W., Shahriari, M., Shelest, E., Silva-Franco, F., Soanes, D., Syed, K., Tagua, V.G., Talbot, N.J., Thon, M.R., Tice, H., de Vries, R.P., Wiebenga, A., Yadav, J.S., Braun, E.L., Baker, S.E., Garre, V., Schmutz, J., Horwitz, B.A., Torres-Martínez, S., Idnurm, A., Herrera-Estrella, A., Gabaldón, T., Grigoriev, I.V., 2016. Expansion of signal transduction pathways in fungi by extensive genome duplication. *Curr Biol.* 26, 1577-1584. <https://doi.org/10.1016/j.cub.2016.04.038>.

Galgóczy, L., Nyilasi, I., Papp, T., Vágvölgyi, C., 2009. Are statins applicable for the prevention and treatment of zygomycosis? *Clin. Infect. Dis.* 49, 483-484. <https://doi.org/10.1086/600825>.

Higgins, V.J., Beckhouse, A.G., Oliver, A.D., Rogers, P.J., Dawes, I.W., 2003. Yeast genome-wide expression analysis identifies a strong ergosterol and oxidative stress response during the initial stages of an industrial lager fermentation. *Appl. Environ. Microbiol.* 69, 4777-4787. <https://doi.org/10.1128/AEM.69.8.4777-4787.2003>.

Koning, A.J., Roberts, C.J., Wright, R.L., 1996. Different subcellular localization of *Saccharomyces cerevisiae* HMG-CoA reductase isozymes at elevated levels corresponds to distinct endoplasmic reticulum membrane proliferations. *Mol. Biol. Cell* 7, 769-789.

Kuzina, V., Domenech, C., Cerdá-Olmedo, E., 2006. Relationships among the biosyntheses of ubiquinone, carotene, sterols, and triacylglycerols in Zygomycetes. *Arch. Microbiol.* 186, 485-493. <https://doi.org/10.1007/s00203-006-0166-9>

Leal Jr, S.M., Roy, S., Vareechon, C., deJesus Carrion, S., Clark, H., Lopez-Berges, M.S., Di Pietro, A., Schrettl, M., Beckmann, N., Redl, B., Haas, H., Pearlman, E., 2013. Targeting iron acquisition blocks infection with the fungal pathogens *Aspergillus fumigatus* and *Fusarium oxysporum*. *PLoS Pathog.* 9, e1003436. <https://doi.org/10.1371/journal.ppat.1003436>.

Learned, R.M., Fink, G.R., 1989. 3-hydroxy-3-methylglutaryl coenzyme A reductase from *Arabidopsis thaliana* is structurally distinct from the yeast and animal enzymes. *Proc. Nat. Acad. Sci. USA* 86, 2779-2783.

Lee, S.C., Li, A., Calo, S., Heitman, J., 2013. Calcineurin plays key roles in the dimorphic transition and virulence of the human pathogenic zygomycete *Mucor circinelloides*. *PLoS Pathog.* 9, e1003625. <https://doi.org/10.1371/journal.ppat.1003625>.

Lee, S.C., Li, A., Calo, S., Inoue, M., Tonthat, N.K., Bain, J.M., Louw, J., Shinohara, M.L., Erwig, L.P., Schumacher, M.A., Ko, D.C., Heitman, J., 2015. Calcineurin orchestrates dimorphic transitions, antifungal drug responses and host-pathogen interactions of the pathogenic mucoralean fungus *Mucor circinelloides*. *Mol. Microbiol.* 97, 844-865. <https://doi.org/10.1111/mmi.1307>.

Leivar, P., Gonzáles, V.M., Castelas, S., Trelease R.N., López-Iglesias, C., Arró, M., Boronat, A., Campos, N., Ferrer, A., Fernández-Busquets, X., 2005. Subcellular localization of

Arabisopsis 3-hydroxy-3-methylglutaryl coenzyme A reductase. *Plant Phys.* 137, 57-69.

<https://doi.org/10.1104/pp.104.050245>.

Li, C.H., Cervantes, M., Springer, D.J., Boekhout, T., Ruiz-Vazquez R.M., Torres-Martínez, S.R., Heitman, J., Lee, S.C., 2011. Sporangiospore size dimorphism is linked to virulence of *Mucor circinelloides*. *PLoS Pathog.* 7, e1002086.

<https://doi.org/10.1371/journal.ppat.1002086>.

Liscum, L., Finer-Moore, J., Stroud, R.M., Luskey, K.L., Brown, M.S., Goldstein, J.L., 1985. Domain structure of 3-hydroxy-3-methylglutaryl coenzyme A reductase, a glycoprotein of the endoplasmic reticulum. *J. Biol. Chem.* 260, 522-530.

Lovell, S.C., Davis, I.W., Arendall, W.B. 3rd., de Bakker, P.I., Word, J.M., Prisant, M.G., Richardson, J.S., Richardson, D.C., 2003. Structure validation by Calpha geometry: phi,psi and Cbeta deviation. *Proteins* 50, 437-450. <https://doi.org/10.1002/prot.10286>.

Lukács, G., Papp, T., Somogyvári, F., Csernetics, Á., Nyilasi, I., Vágvölgyi, C., 2009.

Cloning of the *Rhizomucor miehei* 3-hydroxy-3-methylglutaryl-coenzyme A reductase gene and its heterologous expression in *Mucor circinelloides*. *Antonie Van Leeuwenhoek* 95, 55-64. <https://doi.org/10.1007/s10482-008-9287-2>.

Macreadie, I.G., Johnson, G., Schlosser, T., Macreadie, P.I., 2006. Growth inhibition of *Candida* species and *Aspergillus fumigatus* by statins. *FEMS Microbiol. Lett.* 262, 9-13. <https://doi.org/10.1111/j.1574-6968.2006.00370.x>.

Marisco, G., Saito, S.T., Ganda, I.S., Brendel, M., Pungartnik, C., 2011. Low ergosterol content in yeast *adh1* mutant enhances chitin maldistribution and sensitivity to paraquat-induced oxidative stress. *Yeast* 28, 263-373. <https://doi.org/10.1002/yea.1844>.

Minder, C.M., Blaha, M.J., Home, A., Michos, E.D., Kaul, S., Blumenthal, R.S., 2012. Evidence-based use of statins for primary prevention of cardiovascular disease. *Am. J. Med.* 125, 440-446. <https://doi.org/10.1016/j.amjmed.2011.11.013>.

Nagy, Á., Vágvölgyi, C., Balla, É., Ferenczy, L., 1994. Electrophoretic karyotype of *Mucor circinelloides*. *Curr. Genet.* 26, 45-48.

Nagy, G., Farkas, A., Csernetics, Á., Bencsik, O., Szekeres, A., Nyilasi, I., Vágvölgyi, C., Papp, T., 2014. Transcription of the three HMG-CoA reductase genes of *Mucor circinelloides*. *BMC Microbiol.* 14, 93. <https://doi.org/10.1186/1471-2180-14-93>.

Nagy, G., Szebenyi, Cs., Csernetics, Á., Vaz, A.G., Tóth, E.J., Vágvölgyi, Cs., Papp, T., 2017. Development of a plasmid free CRISPR-Cas9 system for the genetic modification of *Mucor circinelloides*. *Sci. Rep.* 7, 16800. <https://doi.org/10.1038/s41598-017-17118-2>.

Nicolás, F.E., Vila, A., Moxon, S., Cascales, M.D., Torres-Martínez, S., Ruiz-Vázquez R.M., Garre, V., 2015. The RNAi machinery controls distinct responses to environmental signals in the basal fungus *Mucor circinelloides*. *BMC Genomics* 16, 237. <https://doi.org/10.1186/s12864-015-1443-2>.

Papp, T., Nyilasi, I., Csernetics, Á., Nagy, G., Takó, M., Vágvölgyi, C., 2016. Improvement of industrially relevant biological activities in Mucoromycotina fungi, in: Schmoll, M., Dattenböck, C. (Eds.), *Gene Expression Systems in Fungi: Advancements and Applications*. Springer, 97-118.

Petterson, E.F., Goddard, T.D., Hung, C.C., Couch, G.S., Greenblatt, D.M., Meng, E.C., Ferrin, T.E., 2004. UCSF Chimera--a visualization system for exploratory research and analysis. *J. Comput. Chem.* 13, 1605-1612. <https://doi.org/10.1002/jcc.20084>.

Ruiz-Albert, J., Cerdá-Olmedo, E., Corrochano, L.M., 2002. Genes for mevalonate biosynthesis in *Phycomyces*. *Mol. Genet. Genomics* 266, 768-777. <https://doi.org/10.1007/s004380100565>.

Seong, K., Li, L., Hou, Z., Miles, T., Kistler, H.C., Xu, J., 2006. Cryptic promoter activity in the coding region of the HMG-CoA reductase gene in *Fusarium graminearum*. *Fungal Genet. Biol.* 43, 34-41. <https://doi.org/10.1016/j.fgb.2005.10.002>.

Stermer, B., Bianchini, G.M., Korth, K.L., 1994. Regulation of HMG-CoA reductase activity in plants. *J. Lipid Res.* 35, 1133-1140.

Tashiro, M., Kimura, S., Tateda, K., Saga, T., Ohno, A., Ishii, Y., Izumikawa, K., Tashiro, T., Kohno, S., Yamaguchi, K., 2012. Pravastatin inhibits farnesol production in *Candida albicans* and improves survival in a mouse model of systemic candidiasis. *Med. Mycol.* 50, 353-360. <https://doi.org/10.3109/13693786.2011.610037>.

Valle-Maldonado, M.I., Jácome-Galarza, I.E., Gutiérrez-Corona, F., Ramírez-Díaz, M.I., Campos-García, J., Meza-Carmen, V., 2015. Selection of reference genes for quantitative real time RT-PCR during dimorphism in the zygomycete *Mucor circinelloides*. *Mol. Biol. Rep.* 42, 705-711. <https://doi.org/10.1007/s11033-014-3818-x>.

van Heeswijck, R., Roncero, M.I.G., 1984. High frequency transformation of *Mucor* with recombinant plasmid DNA. *Carlsberg Res. Commun.* 49, 691-702.

Vaupotič, T., Plemenitaš, A. 2007. Osmoadaptation-dependent activity of microsomal HMG-CoA reductase in the extremely halotolerant black yeast *Horstea werneckii* is regulated by ubiquitination. *FEBS Lett.* 581, 3391-3395. <https://doi.org/10.1016/j.febslet.2007.06.038>.

Vaupotič, T., Veranic, P., Petrovic, U., Gunde-Cimerman, N., Plemenitas, A., 2008. HMG-CoA reductase is regulated by environmental salinity and its activity is essential for halotolerance in halophilic fungi. *Stud. Mycol.* 61, 61-66. <https://doi.org/10.3114/sim.2008.61.05>.

Verwaal, R., Wang, J., Meijnen, J-P., Visser, H., Sandmann, G., van den Berg, J.A., van Ooyen, A.J., 2007. High-Level production of beta-carotene in *Saccharomyces cerevisiae* by successive transformation with carotogenic genes from *Xanthophyllomyces dendrorhous*. *Appl. Environ. Microbiol.* 73, 4342-4350. <https://doi.org/10.1128/AEM.02759-06>.

Vincent, J.H., Anthony, G.B., Anthony, D.O., Peter, J.R., Ian, W.D., 2003. Yeast genome-wide expression analysis identifies a strong ergosterol and oxidative stress response during

the initial stages of an industrial large fermentation. *Appl. Environ. Microbiol.* 67, 4777-4787.
<https://doi.org/10.1128/AEM.69.8.4777-4787.2003>.

Wang, G.Y., Keasling, J.D., 2002. Amplification of HMG-CoA reductase production enhances carotenoid accumulation in *Neurospora crassa*. *Metab. Eng.* 4, 193-201.
<https://doi.org/10.1006/mben.2002.0225>.

Xu, D., Zhang, Y., 2011. Improving the physical realism and structural accuracy of protein models by a two-step atomic-level energy minimization. *Biophys. J.* 101, 2525-2534.
<https://doi.org/10.1016/j.bpj.2011.10.024>.

Yan, G-L., Wen, K-R., Duan, C-Q., 2012. Enhancement of β -carotene production by over expression of HMG-CoA reductase coupled with addition of ergosterol biosynthesis inhibitors in recombinant *Saccharomyces cerevisiae*. *Curr. Microbiol.* 64, 159-163.
<https://doi.org/10.1007/s00284-011-0044-9>.

Yang, J., Yan, R., Roy, A., Xu, D., Poisson, J., Zhang, Y., 2015. The I-TASSER Suite: protein structure and function prediction. *Nat. Methods.* 12, 7-8.
<https://doi.org/10.1038/nmeth.3213>.

Fig. 1. The reaction catalyzed by the HMG-CoA reductase. Abbreviations: HMG-CoA, 3-hydroxy-3-methylglutaryl coenzyme A; HS-CoA, coenzyme A; NADP⁺, nicotinamide adenine dinucleotide phosphate; NADPH, reduced NADP.

Fig. 2. Genome editing strategy designed to disrupt the *hmgR* genes of *Mucor circinelloides* using the CRISPR-Cas9 method. HDR was performed using the disruption cassette/template DNA containing either the *pyrG* or the *leuA* gene as selection markers. Positions of the primers used to analyze or amplify the constructs are presented (for the nucleic acid sequences of the primers, see Supplementary Table S1). TGG indicates the PAM sequence while the arrows show the orientations of the primers.

Fig. 3. Light and fluorescent microscopy examination of the subcellular localization of the HmgR:GFP fusion proteins. The scale bar indicates 20 μ m.

Fig. 4. PCR analysis of the transformants (A, C, E, G, I) and the relative transcript levels of the *hmgR* genes in the mutants compared to the original MS12 strain (B, D, F, H, J).

For panels A, C, E, G and I, M: GeneRuler 1 kb DNA ruler (Thermo Scientific). In the PCR experiments, the primer pairs H1cDNS1 - H1cDNS8 (A), H2cDNS1 - H2cDNS8 (C) and H3cDNS1 - H3cDNS8 (E) were used for *hmgR1*, *hmgR2* and *hmgR3*, respectively. For the primer sequences and the primers used in the qRT-PCR experiments, see Supplementary Table S1. In the panels B, D, F, H and J, relative transcript level of the *hmgR* genes in the mutants are compared to those in the original strain: transcript level of each gene measured in the MS12 was taken as 1. The presented values are averages of three independent experiments (error bars indicate standard deviation). Relative transcript levels significantly different from the value taken as 1 according to the paired t-test are indicated with * or ** (* p <0.05,

** $p < 0.01$). Pictures presented in panels A, C, E, G and I were cropped from the same gel photo; the original undivided, full-length photo is included in the Supplementary Information file (Supplementary Fig. S1).

Fig. 5. Percentage of the metabolically active spores (A) and the germinating sporangiospores (B) determined for the *hmgR* disruption mutants and the original MS12 strain of *Mucor circinelloides*. The presented values are averages of three independent experiments (error bars indicate standard deviation). Germ tube development was counted after cultivations for 5 h at 25 °C. Values followed by * and ** significantly differed from the corresponding value of the MS12 strain according to the paired *t*-test (* $p < 0.05$, ** $p < 0.01$).

Fig. 6. Colony diameters of the *hmgR* disruption mutants and the original MS12 strain of *Mucor circinelloides* at different temperatures. The presented values are averages; colony diameters were measured during three independent cultivation (error bars indicate standard deviation). Values followed by * and ** significantly differed from the corresponding value of the MS12 strain according to the paired *t*-test (* $p < 0.05$; ** $p < 0.01$).

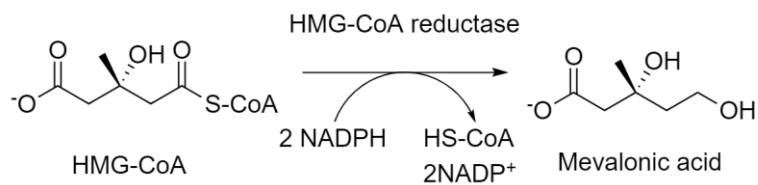
Fig. 7. Predicted tertiary structures of the proteins HmgR1, HmgR2 and HmgR3 of *Mucor circinelloides*. The conserved HMG-CoA and NADPH binding sites are indicated by yellow and red colors, respectively. Sterol binding transmembrane regions are marked with magenta. Contents of the .pdb files are available in Supplementary Dataset S1-S3.

Fig. 8. Summary of the processes, which were found to be affected by the activity of the three *hmgR* genes of *Mucor circinelloides*.

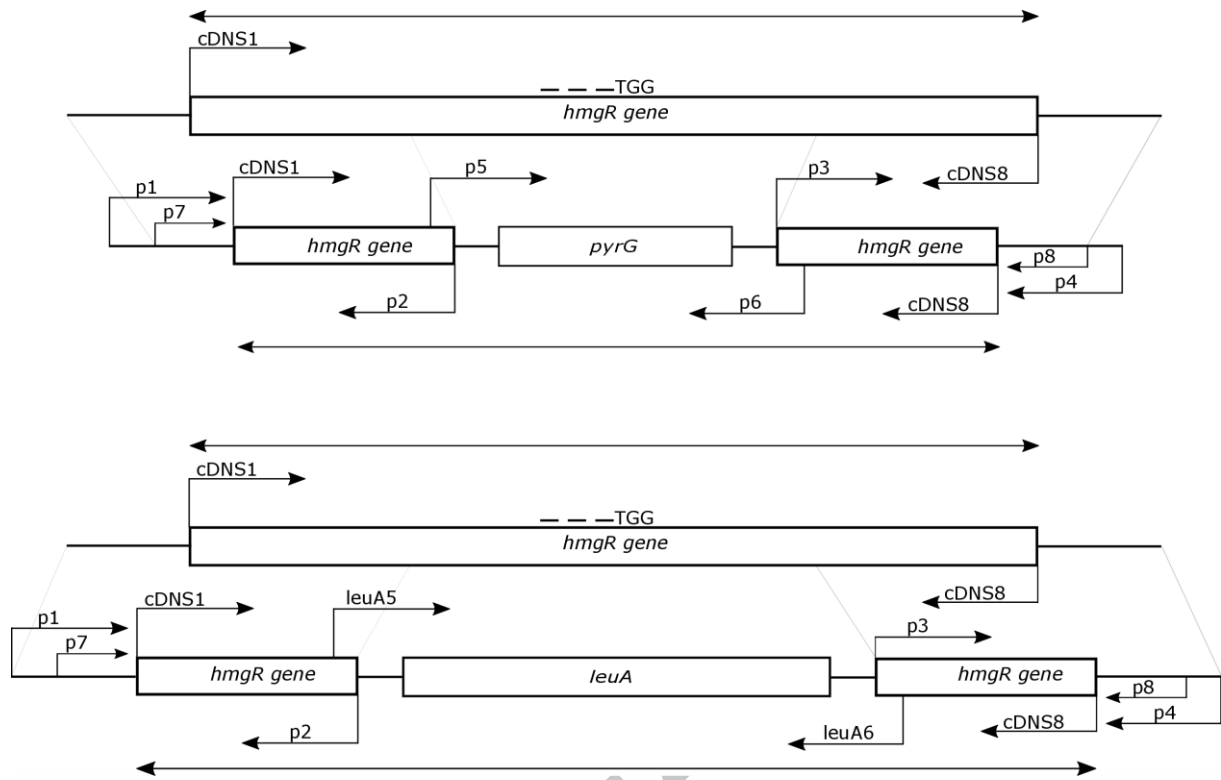
Table 1

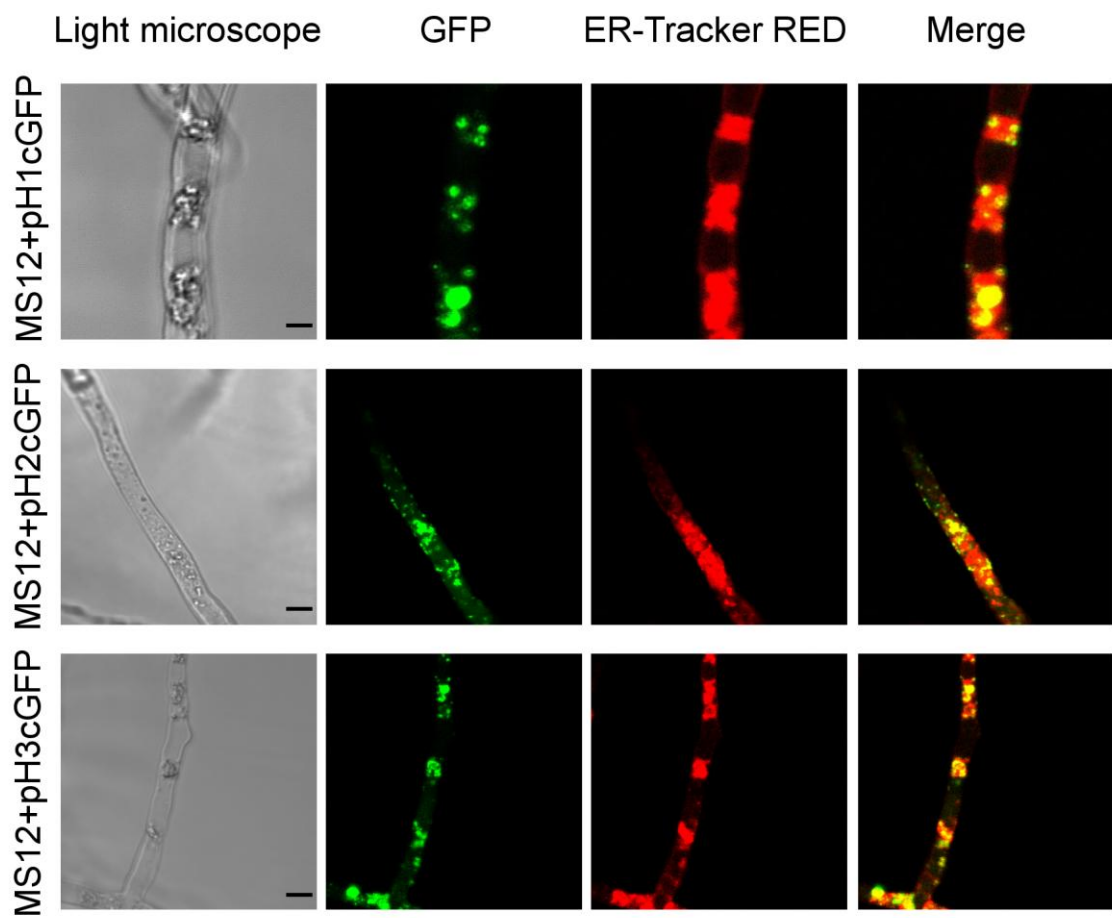
Minimal inhibitory concentrations (MIC) of three statins ($\mu\text{g/ml}$) and H_2O_2 (mM) against the transformants and the parental *M. circinelloides* MS12 strain.

Strains	Fluvastatin	Atorvastatin	Rosuvastatin	H_2O_2
MS12	4	16	32	>10
MS12- ΔhmgR1	4	16	32	9
MS12- ΔhmgR2	2	8	16	8
MS12- ΔhmgR3	1	4	8	8
MS12- $\Delta\text{hmgR1-}\Delta\text{hmgR2}$	2	8	16	7
MS12- $\Delta\text{hmgR1-}\Delta\text{hmgR3}$	1	4	8	5

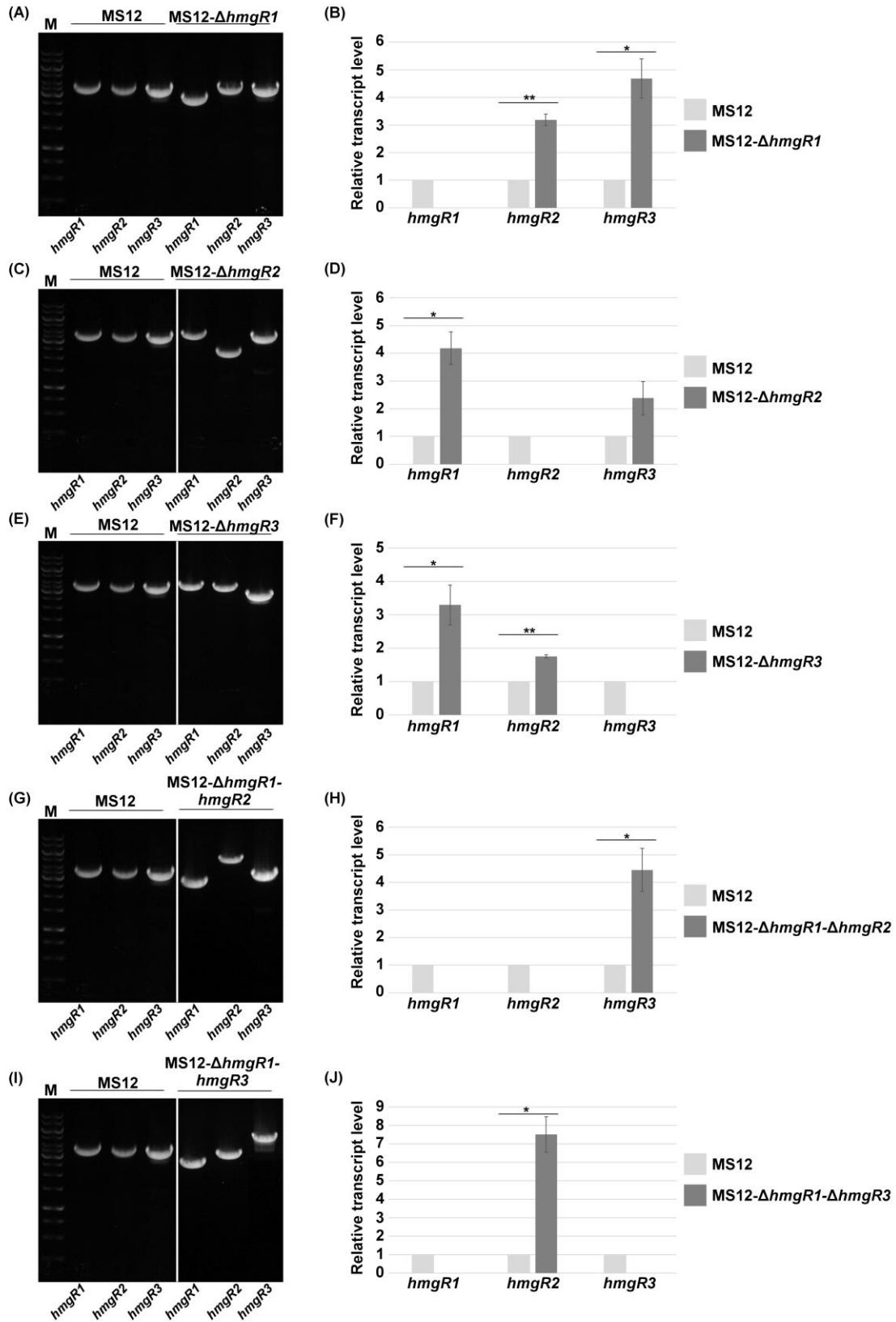


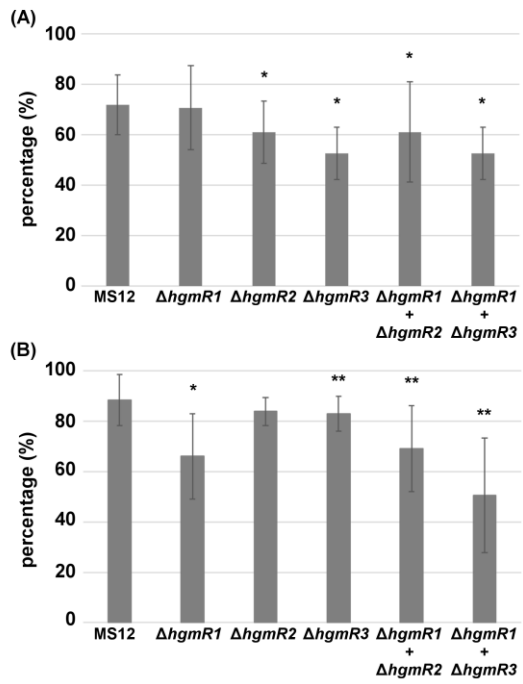
ACCEPTED MANUSCRIPT

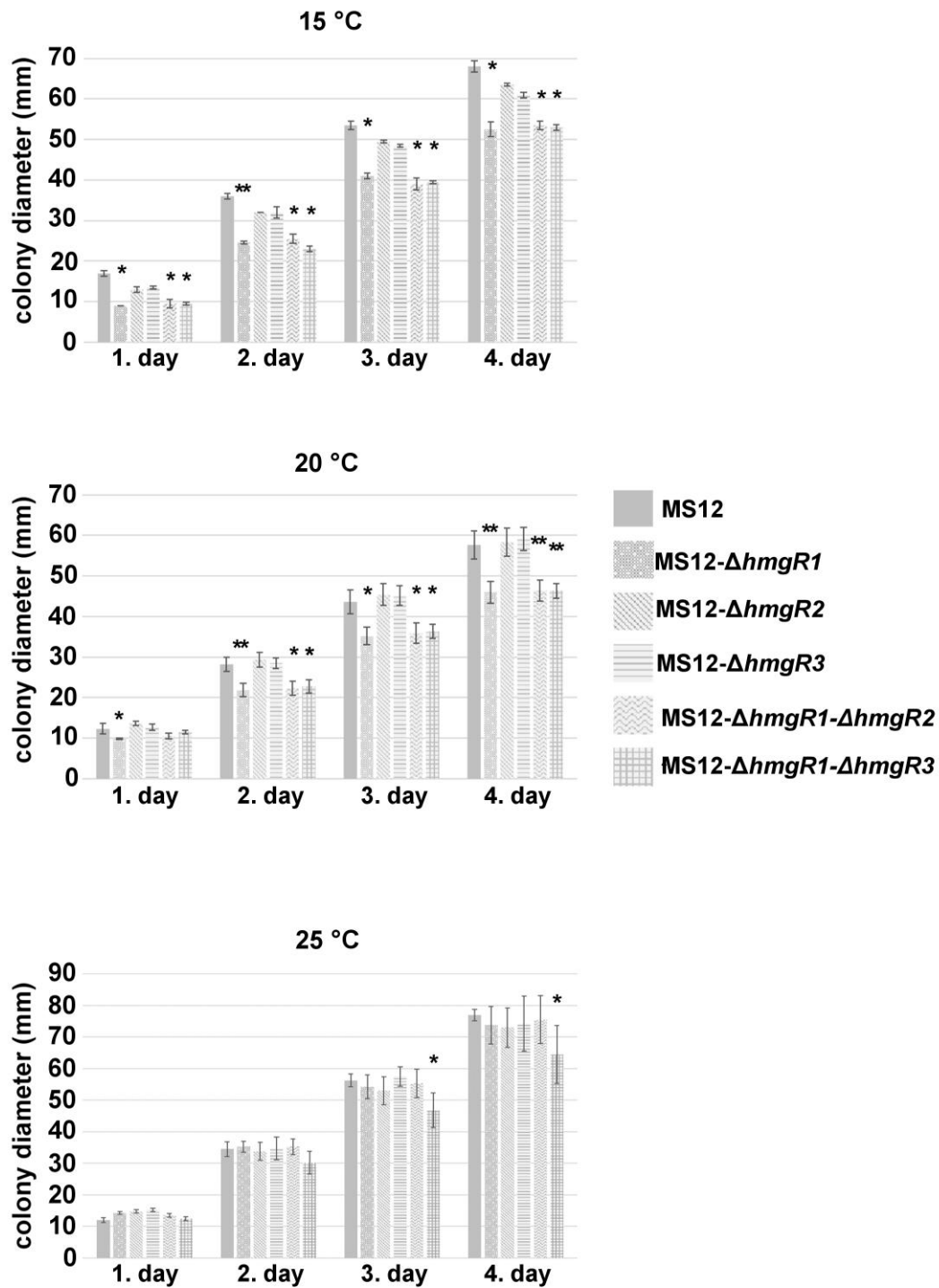




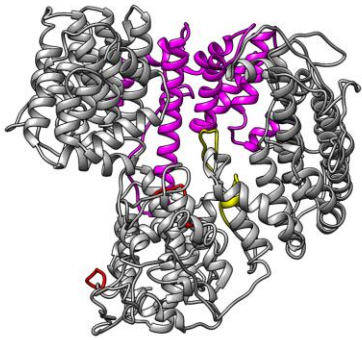
ACCEPTED



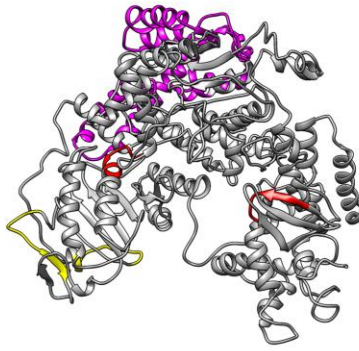




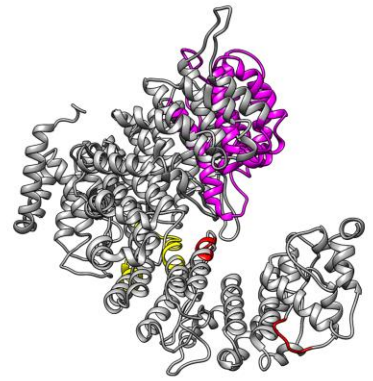
HmgR1



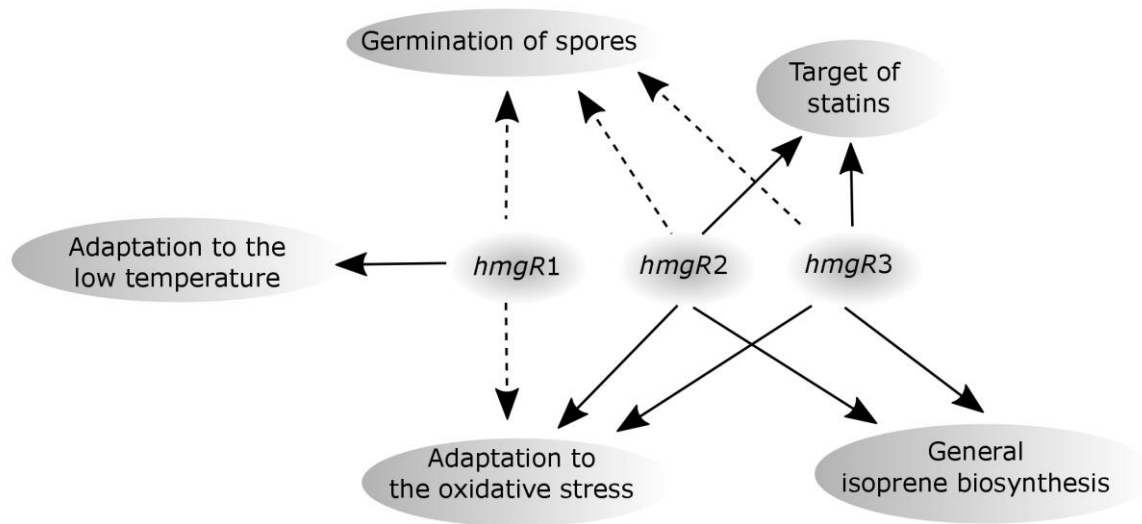
HmgR2



HmgR3



ACCEPTED MANUSCRIPT



ACCEPTED MANUSCRIPT

Highlights:

Mucor circinelloides HMG-CoA reductase genes were disrupted by the CRISPR-Cas9 method

Function of *hmgR2* and *hmgR3* are overlapping and involved in the terpene biosynthesis

HmgR2 has a special role in the ergosterol biosynthesis

Disruption of the *hmgR1* gene caused a reduced growth at lower temperatures

By confocal microscopy, all three enzymes were localized in the endoplasmic reticulum

ACCEPTED MANUSCRIPT